Int. J. Heat Mass Transfer. Vol. 36, No. 3, pp. 565–576, 1993
Printed in Great Britain

0017-9310/93 $6.00+0.00
Pergamon Press Ltd

Heat transfer and pressure drop in large pitch spirally indented tubes

C. B. PANCHAL† and D. M. FRANCE‡
†Argonne National Laboratory, Argonne, IL 60439, U.S.A.
‡University of Illinois at Chicago, Chicago, IL 60680, U.S.A.

(*Received* 23 *December* 1991 *and in final form* 15 *April* 1992)

Abstract—Heat transfer and pressure drop experiments are performed with water, at atmospheric pressure in the Prandtl number range 3.6–8.8, flowing in spirally indented tubes for heat exchanger applications. Large pitch geometries are studied which minimize pressure drop. The pitch to indentation height ratio is in the range of 23.7–120, which is beyond the range generally considered in previous investigations. Four tubes are tested with the indentation height to diameter ratios of 0.0075, 0.021, 0.038 and 0.0 (plain). The tubes are tested in a counter-current flow configuration that produces results directly applicable to heat exchanger design applications. A data reduction technique is developed that is applicable to an arbitrarily augmented tube, and it is verified with the plain-tube data. Heat transfer and pressure drop results from the spirally indented tubes are compared to extensions of correlations for similar geometries and to limited data available at large pitches.

INTRODUCTION

MANY TYPES of surface enhancements have been studied for the augmentation of forced convection heat transfer inside tubes. A particularly cost-effective enhancer is produced by indenting the outside of the tube in a spiral pattern, producing an internal indentation with a relatively smooth profile. Such spirally indented tubes have been studied for a variety of applications and have also been called rope tubes or indented tubes. It should be recognized that the heat-transfer enhancement achieved by means of surface effects at the boundary layer is generally associated with increase in pressure drop. Pressure sensitive applications such as heat exchangers for power plant bottoming cycles, energy cogeneration and ocean thermal energy conversion may be unable to make use of many surface enhancements. The purpose of this investigation was to study the use of spirally indented tubes for low pressure drop applications. Both the smooth shape of the indentation in these tubes and the large pitches studied contribute to pressure drop minimization.

Surface enhancement for low pressure drop cases is particularly attractive for use with fluids having Prandtl numbers greater than unity. A low height indentation can potentially upset the thermal boundary layer without significantly disturbing the hydrodynamic boundary layer. The result of such an occurrence would be an increase in heat transfer efficiency without a large increase in pressure drop or pumping power. Indented tubes were used in this study for enhancing heat transfer to water flowing turbulently in tubes in the Prandtl number range of 3.6–8.8. Since the pitch of the single start spiral indentation was chosen to be relatively large to maintain minimum pressure drop, the geometry studied was outside the pitch range of the majority of previous tubes tested and reported in the engineering literature. A notable exception exists with the data of ref. [1] where the spirally indented tubes tested included tubes identical to those used in this study. The limited data available [1] in the Reynolds number range of interest were utilized in this work. An extensive compilation of general data was also given in ref. [1] which included spirally indented tubes and other similar enhancers like transverse ribs, square ribs and coiled wire inserts. A subset of that data was developed [2] specifically for spirally indented tubes.

The experimental approach taken in this investigation was to use a heat-exchanger test section in which the test fluid flowing in the tube was heated by a second fluid flowing counter-current in the surrounding annulus. This approach represents more prototype heating conditions than that for the more common approach of direct heating of the tube wall. The direct heating approach presents two important experimental problems. Heating is not uniform in the tube wall due to the tube manufacturing process that may produce a different thickness in the indentation area relative to the remainder of the tube. Residual stresses from the manufacturing process also contribute to this non-uniformity of heating. The second problem area occurring in direct heating of indented tubes is related to the measurement of tube wall temperature. Application of results to a heat exchanger generally requires an average temperature between the indented and plain portions of the tube. This application poses problems in the selection of locations at which to measure wall temperatures. The experimental approach used in this study, employing a heat exchanger directly, was not subject to either of the

NOMENCLATURE

A	area [m^2]
D	test section tube inside diameter before indentation [m]
e	indentation height [m]
e^+	roughness Reynolds number
f	Fanning friction factor
G	heat-transfer similarity parameter
h	heat-transfer coefficient [kW m^{-2} K^{-1}]
k_w	thermal conductivity of test section wall [kW m^{-1} K^{-1}]
LMTD	log mean temperature difference
Nu	Nusselt number
n	indentation shape factor
Pr	Prandtl number
p	indentation pitch [m]
$\dot{q}$	heat-transfer rate [kW]
r	radius [m]
R	friction similarity function
R^*	ratio of annulus diameters (>1.0)
Re	Reynolds number
R_w	thermal resistance of test section tube wall [m^2 K kW^{-1}]
St	Stanton number
T	temperature [°C]
U_o	overall heat-transfer coefficient referenced to the outside surface of the test section tube [kW m^{-2} K^{-1}].

Greek symbols

α	indentation helix angle with tube axis [deg]
β	indentation contact angle [deg]
γ	exponent on tube-side Reynolds number
δ	exponent on annulus-side Reynolds number.

Subscripts

i	tube-side or inner surface of test section tube
o	annulus-side or outer surface of test section tube
s	plain surface.

problems of uniform heating or tube wall temperature measurement. The experimental technique used in the present analysis followed the Wilson technique [3]; however, a new approach was required for the enhanced tubes where the Reynolds number exponent is not known precisely.

Experiments were performed with a plain (non-indented) tube and three spirally indented tubes with indentation heights of $e/D = 0.0075$, 0.021 and 0.038. The tube diameter of 23.8 mm and the pitch were kept constant among the enhanced tubes tested yielding a constant pitch to diameter ratio, $p/D = 0.9$. Results were compared to available correlation equations for heat transfer and friction factor in indented tubes. Most of the data used for the literature correlations were outside the range of this investigation of $p/e = 23.7$–120. Consequently, the literature correlations were generally tested in an extrapolated range of conditions.

EXPERIMENTAL APPARATUS

Facility

Thermal/hydraulic performance measurements were carried out in the Heat Exchanger Test Facility at Argonne National Laboratory. A single channel heat transfer test loop was used, a schematic flow diagram of which is shown in Fig. 1. The test apparatus has two closed loops for circulation of warm water and cold water. As shown in Fig. 1, the test apparatus was designed to control fluid temperatures within about 0.1°C for both inside and outside flow streams during a given series of tests. The warm water loop consists of a storage tank with circulation pump, electric heater, flowmeter and control valves. The rate of heat transfer was manually adjusted by controlling the electric power to the heater using a rheostat. Further control of inlet temperature was done by an automatic proportionate/integral temperature controller which adjusted current to the control heater. Heat was rejected to chilled water provided either by a chiller or by an in-house supply at about 12°C depending upon the test unit operating temperature. The cold water inlet temperature to the test unit was adjusted to a predetermined value by controlling flow to the chilled water heat exchanger. Warm water flowed inside the spirally indented tubes and cold water flowed outside.

Flow rate capacities of the cold and warm water loops were in the range of 2–12 l s^{-1}. Storage capacities of the cold- and warm-water tanks were 75 and 1500 l, respectively. The test range of heat duty was 1 and 8 kW. Both storage tanks were open to the atmosphere and the low pressure allowed the use of plastic pipes and fittings for the flow systems.

Temperatures, flow rates and pressure drops were measured for both flow streams at inlets and outlets to the test section. Quartz crystal thermometers with an estimated accuracy of 0.01°C were used for measurement of inlet and outlet temperatures and for temperature changes across the test section. They were factory calibrated and, before each series of experiments, a single point check was made using an icebath. Previous studies [4] have shown that this method provides the high accuracy required for the low temperature differences of the present exper-

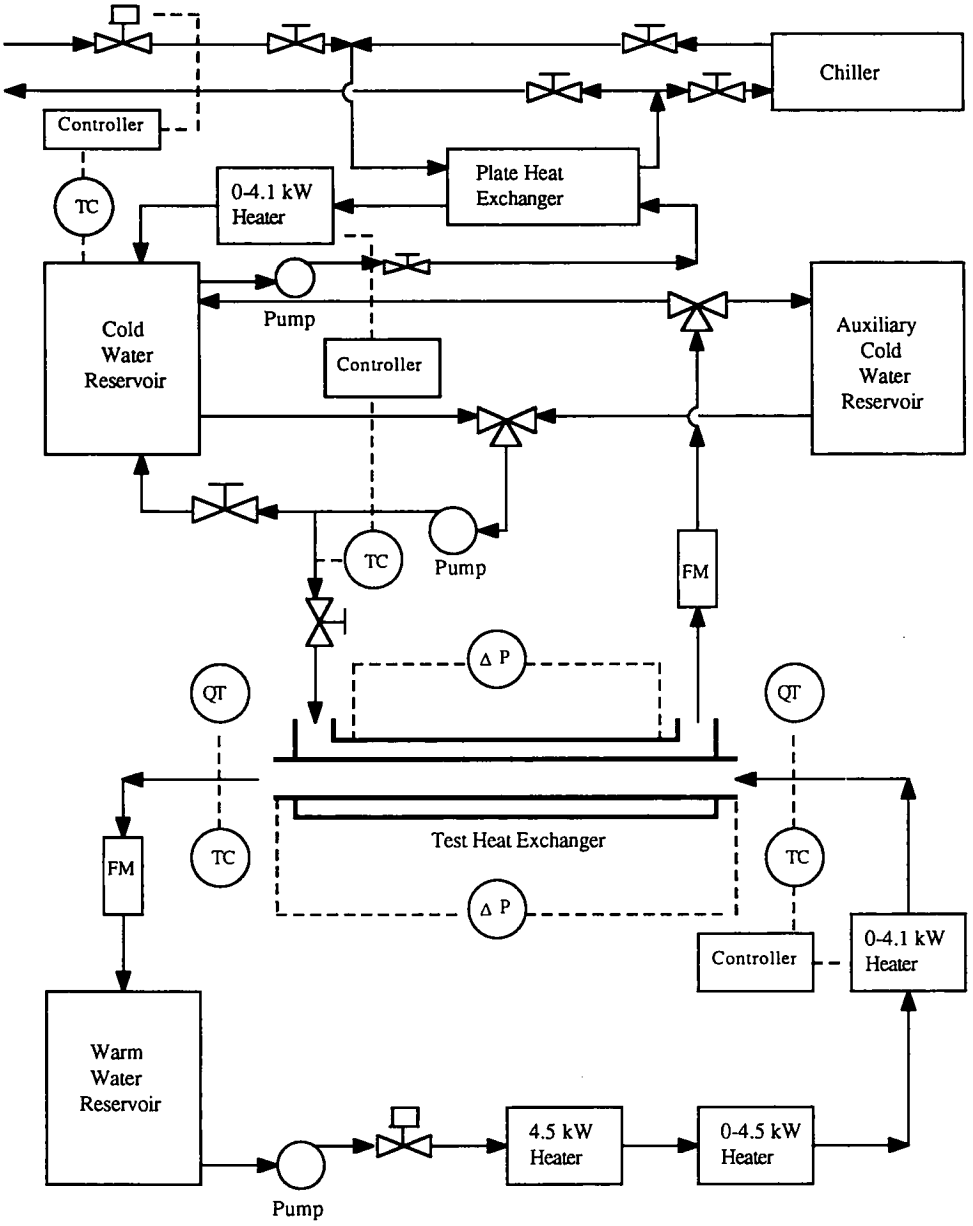

FM = Turbine Flowmeter QT = Quartz Thermometer TC = Thermocouple Δ P = Strain Guage Pressure Sensor

FIG. 1. Flow schematic of the test facility.

imental work. Water flow rates were measured by turbine flowmeters. Each flowmeter was calibrated using a calibrated tank and repeated tests showed an accuracy of better than 1% of readings. Pressure drop measurements were done by strain gauge pressure sensors. They were calibrated after installation in the system by providing a measured water column on one side of the differential pressure sensor and atmospheric conditions on the other side. All calibration data were stored in the data acquisition computer. Heat balance comparisons between tube and annulus flow streams were made during all tests and they agreed within 5% for most experiments.

The test facility's computerized data acquisition system was used to read the individual instrument outputs, apply calibration factors to the data, carry out engineering calculations, display readings on the monitor and produce a hard copy of all measured and calculated quantities. The computer sampled all the data periodically at a rate determined by the operator (generally four to five times per minute). Running averages of various parameters were made and after

Table 1. Dimensions for the test section

Parameter		Value	Units
Heated length		1.52	m
Tube diameter		24.0	mm
Wall thickness		0.71	mm
Annulus diameter		50.8	mm
Heat transfer area:			
inside		0.115	m^2
outside		0.121	m^2
Enhancement:			
pitch		19.1	mm
height	tube 1	0.15	mm
	tube 2	0.31	mm
	tube 3	0.51	mm
	tube 4	0.91	mm

a given number of data sets (usually 20–30) results were displayed and printed. This procedure followed the attainment of steady-state conditions that were assumed to be achieved when key temperatures and flow rates were within measurement accuracies for greater than 15 min. The raw data were transferred to the mainframe computer for the detailed analysis.

Test unit

The test unit consisted of a double pipe heat exchanger. The outer pipe was used separately with three spirally indented test section tubes. The inlets and outlets of the test unit were instrumented as discussed previously. Special consideration was given to the installation of the sensors. The bulbs of the quartz thermometers were installed in a manner that allowed water to flow completely around them. This configuration produced high accuracy readings of fluid temperatures. Small pressure taps were used for the differential pressure sensors and care was taken to ensure that they were flush with the inside surface. This configuration minimized the potential for error that can be introduced into the system by vortex formation near the pressure tapes.

Three large pitch tubes were manufactured by Wolverine of UOP, Inc. for this study; dimensions are given in Table 1 and a photographic view of one of the three test sections is shown in Fig. 2. Flow inside the tubes was allowed to develop in a plain, straight upstream section. Flow entered the annulus through a 90° bend and provision was made for this flow to develop hydrodynamically before heat transfer started. Insulating Teflon tapes of 150 mm length were installed at both the inlet and outlet of the test section to minimize entrance and exit flow effects on the heat transfer.

EXPERIMENTAL TECHNIQUE AND DATA ANALYSIS

Approach

All tests were performed at steady state with the test unit operating as a counter-flow heat exchanger whether the test section tube was spirally indented or plain. The rate of heat transfer was determined from the product of the mass flow rate and the enthalpy change for each of the liquid streams, and the log mean temperature difference (LMTD) was used to determine the overall heat-transfer coefficient. The LMTD result for a single pass, counter-flow, shell and tube heat exchanger is applicable to the experiments of this study. The inherent assumptions in the LMTD result are constant fluid and solid properties and constant heat-transfer coefficients along the length of the test unit for any single steady-state test. The constant property criterion was met by controlling the total temperature change of each fluid to be less than 2–3°C in all tests performed. The Reynolds and Prandtl numbers were also relatively constant due to this temperature change control that was a necessary condition for meeting the criterion of constant heat-transfer coefficients. The unheated flow lengths (>20 hydrodynamic lengths) in the test unit approaching the heat-transfer surface were provided specifically for allowing the flows to develop fully from a hydrodynamic standpoint. This condition was also important in satisfying the constant heat-transfer coefficient criterion.

The LMTD result for the integrated energy equation may be written as

$$\dot{q} = U_o A_o \,\mathrm{LMTD}. \tag{1}$$

The overall heat-transfer coefficient based on the outside surface area of the tube is given as

$$\frac{1}{U_o} = \frac{1}{h_o} + \frac{A_o}{A_i} R_w + \frac{A_o}{A_i h_i} \tag{2}$$

and the tube wall resistance is

$$R_w = \frac{r_i \ln (r_i/r_o)}{k_w}. \tag{3}$$

In applying the results of equations (1)–(3) to the tests of this study, the rate of heat transfer and LMTD in equation (1) were determined from the measurements of each steady-state test. At this point, the inside heat-transfer coefficient, h_i, could be determined if the outside coefficient, h_o, was known. Rather than using a value from a heat-transfer correlation for h_o with its inherent inaccuracy, the Wilson plot technique [3] was adapted to determine h_o experimentally.

A series of tests was performed in which the following parameters were held very close to constant: annulus fluid flow rate and temperature and tube fluid temperatures. The only variable among the tests of a single test series was the mass flow rate on the tube side. Under these conditions, equation (2) may be rewritten for application to a test series as

$$\frac{1}{U_o} = C_1 + C_2 Re^{-\gamma} \tag{4}$$

where

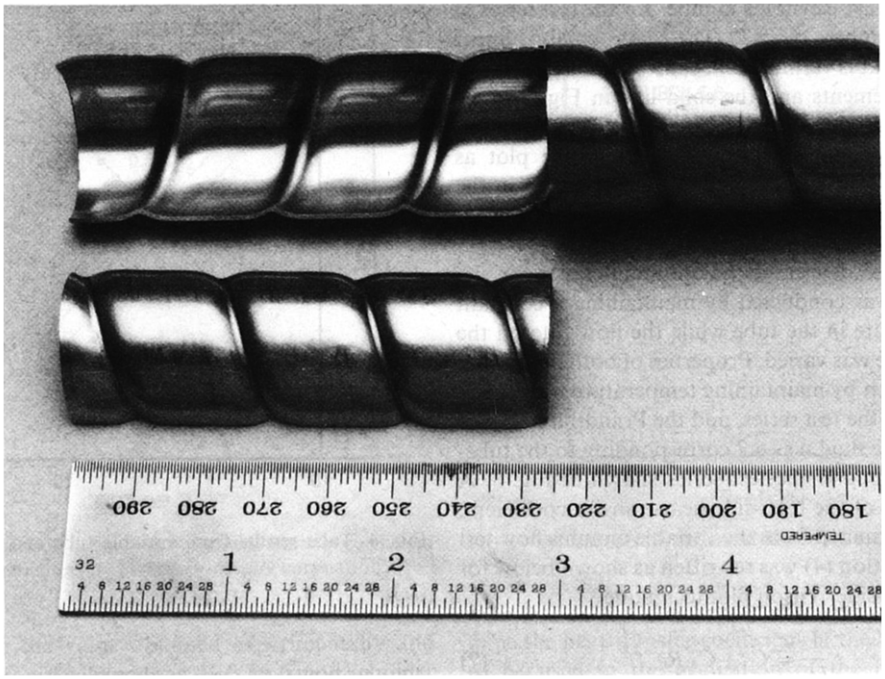

FIG. 2. Photographic view of the test section.

$$C_1 = \frac{1}{h_o} + \frac{A_o}{A_i} R_w \tag{5}$$

$$h_i = \frac{A_o}{A_i C_2} Re^{\gamma}. \tag{6}$$

Parameters C_1, C_2 and γ are all constant for a test series, and for constant Prandtl number, h_i is assumed to have the form of equation (6). In the usual Wilson technique procedure, constants C_1 and C_2 are determined from the linear regression analysis of equation (4). The Reynolds number exponent, γ, must be specified for the procedure. In the case of a plain tube, the choice of γ in the range of 0.8–0.9 is common based on both analysis and extensive experiments reported in the literature. With γ specified, the regression analysis can be performed on the plain tube data; the constant C_1 can be determined and the value of h_o calculated. A problem arises using this procedure for the spirally indented tubes since there is no specific guidance for the choice of the exponent, γ. Thus, as a part of this study, the Wilson technique was extended to include spirally indented tubes. Specifically, a technique was developed for determining the Reynolds number exponent, γ, for an arbitrary channel.

Once the exponent, γ, was specified, the procedure for calculating h_o was the same for both spirally indented and plain tubes. A key feature of the present analysis is that, after h_o was determined in this manner, equation (6) was abandoned. The assumption of a form of the inside heat-transfer coefficient, h_i, was used only in obtaining the value of h_o for the test series. Subsequently, values of h_i were calculated for each test of the series from equation (2). Some researchers have used equation (6) for determining h_i, however, such a procedure introduces data smoothing unnecessarily.

Plain tube

The technique for determining the Reynolds number exponent, γ, was tested by using the data from the plain tube for which γ was known from commonly used heat-transfer correlations. Four series of plain tube tests were performed for this purpose, each consisting of 8 or 9 individual tests. The four test series covered the Prandtl number in the range of 3.6–9.5. A typical result of the Wilson plot method is shown in Fig. 3 where the overall heat-transfer coefficient is

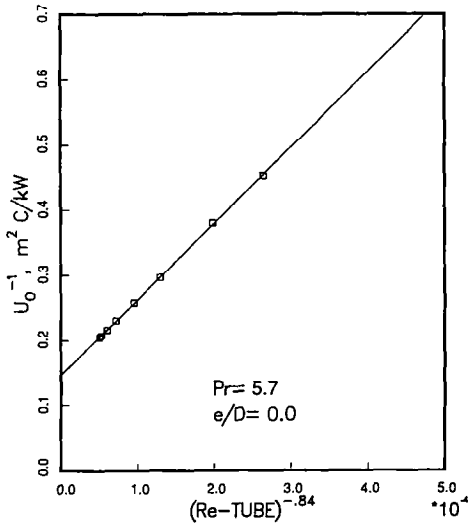

FIG. 3. The Wilson plot showing the overall heat-transfer coefficient linearity.

plotted against Reynolds number for the test series of Prandtl number of 5.7. The data exhibit linear behavior that is verification of the overall accuracy of the measurements and the solid line in Fig. 3 is the result of linear regression analysis. The Reynolds number exponent of 0.84 was used in the plot as indicated. Similar linear trends were observed in the results of the other three test series of Prandtl numbers of 3.6, 8.2 and 9.5.

In order to determine the optimum choice for γ, a test series was conducted by maintaining a constant fluid flow rate in the tube while the flow rate on the annulus side was varied. Properties of both fluids were kept constant by maintaining temperature within 1°C throughout the test series, and the Prandtl number of the tube-side fluid was 5.7 corresponding to the tube-side conditions of the test series shown in Fig. 3. A single value of the tube-side heat-transfer coefficient, h_i, was determined from the variable annulus flow test series. Equation (4) was rewritten as shown below for the annulus-side Wilson plot technique

$$\frac{1}{U_o} = C_3 + C_4 Re_o^{-\delta} \tag{7}$$

where

$$C_3 = \frac{A_o}{A_i h_i} + \frac{A_o}{A_i} R_w \tag{8}$$

and

$$h_o = \left(\frac{1}{C_5}\right) Re^{\delta}. \tag{9}$$

As for the tube-side analysis, the form of the annulus heat-transfer coefficient was assumed to be equation (9) for constant Prandtl number and a value of the exponent δ was specified prior to performing linear regression analysis on the data. It yielded a C_3 value from which a single value of h_i for the variable annulus flow test series was obtained from equation (8). The tube-side Nusselt numbers are presented in Fig. 4 from the variable tube flow and variable annulus flow test series performed at a tube-side Prandtl number of 5.7. The variable tube-side flow rate tests of Fig. 3 are shown as open symbols denoted 'tube test' in Fig. 4. The closed symbol corresponds to the single tube-side Nusselt number result obtained from the variable annulus flow rate test series, denoted 'annulus test' in Fig. 4.

The comparison of tube-side heat-transfer prediction shown in Fig. 4 is sensitive to the value of the Reynolds number exponents used in the data reduction. Combinations of γ and δ in the range 0.75–0.9 were tested with γ not necessarily equal to δ, and the best agreement was obtained with $\gamma = \delta = 0.84$ as shown in Fig. 4. For a selected value for γ, δ was varied until the single point obtained from the linear regression of the annular flow data fell on the curve for the tube-side Nusselt number as shown in Fig. 4. However, a similar agreement might not occur for the annular flow data such as shown in Fig. 5. Therefore, another value for γ was taken, and the procedure was repeated. This iterative procedure was continued until agreement of the data as shown in Figs. 4 and 5 was obtained.

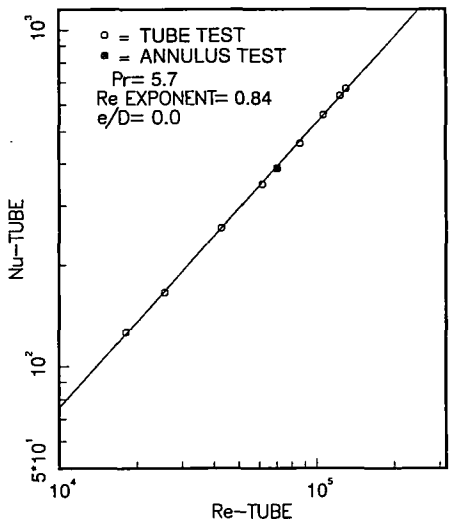

FIG. 4. Tube results from variable tube and annulus flow tests.

Once $\gamma = 0.84$ was determined, a value of h_o was calculated for a given test series. Equation (3) was then used to determine h_i for each test of the series that became the experimental results. In order to compare the experimental data with the literature data, an accepted value of γ was obtained from the commonly used Petukhov–Popov [5] correlation. The Reynolds number dependence of the correlation was cast into the form, Re^{β}, and β was evaluated over the parameter range of this study to be about 0.84. This exponent

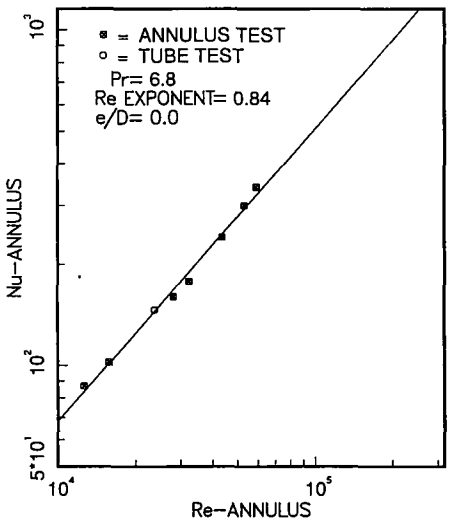

FIG. 5. Annulus results from variable tube and annulus flow tests.

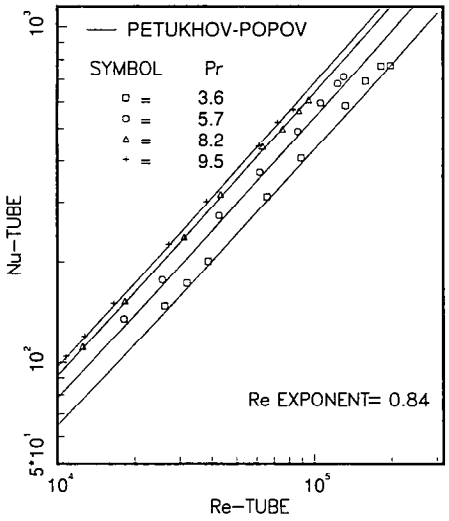

FIG. 6. Comparison of the plain-tube heat-transfer coefficient with predictions by Petukhov–Popov correlation.

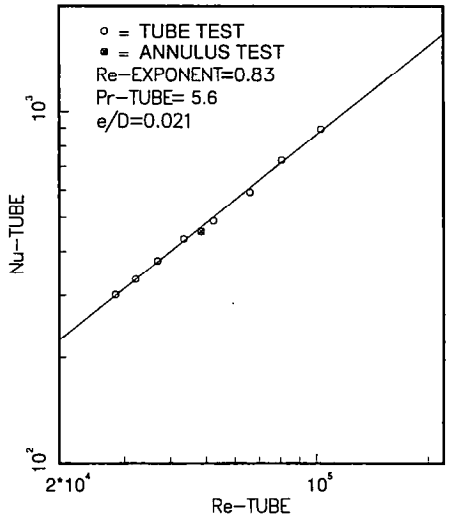

FIG. 7. Typical spirally indented tube data reduction results.

agrees with the value obtained experimentally and is higher than the exponent of 0.80 found in older correlations, e.g. Sieder–Tate or Dittus–Boelter. The plain tube data were compared directly to predictions of the Petukhov–Popov correlation and good agreement is shown in Fig. 6.

Spirally indented tubes

The technique presented for determining the Reynolds number exponent for data reduction purposes for an arbitrary tube successfully predicted the plain tube exponent of 0.84. This technique, of combining variable tube and annulus flow tests to determine the appropriate exponent, was used for the analysis of data from the three spirally indented tubes tested.

Variable tube flow and variable annulus flow tests were performed at tube-side Prandtl numbers of 3.6, 5.6 and 8.8 using each of the spirally indented tubes. In reducing the data, according to the technique developed from the plain tube tests, values of γ and δ were used in the range of 0.80–0.88 with γ not necessarily equal to δ. However, their values were close to each other; therefore, both exponents were assumed to be equal in the analysis. The overall agreement between h_i and h_o predicted for variable tube flow and variable annulus flow tests was obtained for each tube as follows:

$$e/D = 0.0075, \quad \gamma = \delta = 0.84;$$

$$e/D = 0.021, \quad \gamma = \delta = 0.83;$$

$$e/D = 0.038, \quad \gamma = \delta = 0.80.$$

A typical Nusselt number comparison is shown in Fig. 7 for $e/D = 0.021$.

RESULTS AND DISCUSSION

Annulus heat transfer

The purpose of the data reduction technique developed in this study was to experimentally determine the heat-transfer coefficient of the annulus fluid to be used in the evaluation of the tube-side coefficients. In the case of the plain tube, the annulus coefficient, thus determined, was compared to predictions from an established annulus correlation equation [6] that was reported [7] to be in good agreement with independent experimental data

$$Nu = 0.02\, Re^{0.8}\, Pr^{1/3} (R^*)^{0.53} \qquad (10)$$

where Nu and Re are based on the annulus hydraulic diameter. The good agreement obtained between this correlation, equation (10), and the plain-annulus results of this study, as shown in Fig. 8, serves to support the accuracy of the annulus heat-transfer coefficient obtained from the data reduction technique developed. Predictions of the Petukhov–Popov tube

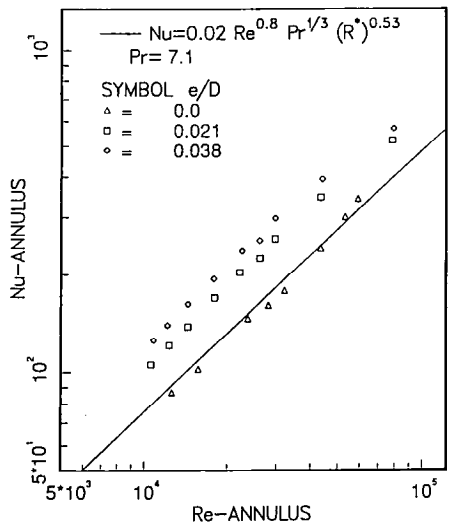

FIG. 8. The annulus heat-transfer coefficient as a function of Reynolds number and indentation height.

correlation, applied to the annulus using the hydraulic diameter, were within approximately 12% of the data. This result is also supportive of the technique developed.

The annulus heat-transfer results for spirally indented tubes are shown in Fig. 8. An average value of the enhancement factor (ratio of enhanced to plain surface heat-transfer coefficient) for $e/D = 0.021$ was about 1.32 as compared to that for the tube-side value of 1.50. However, an incremental enhancement for $e/D = 0.038$ as compared to that for $e/D = 0.021$ was less significant.

Tube friction factor

Pressure drop measurements from the four tubes tested in this study were converted to Fanning friction factors and compared to the prediction of several indented tube correlations. Withers' equation [8] was chosen for comparison because it was developed for spirally indented tubes similar to those of this study although the pitches and indentation heights differed. The data base for the correlation had a minimum indentation height, e/D, approximately twice the value of the minimum of this study and the pitch, p/D, was less than 60% of the pitch of this study. Withers' equation overpredicted all but the tube data and the discrepancy increased with indentation height to over 50% at $e/D = 0.038$. It should be noted that Withers' equation is based on two parameters that were presented graphically [8]; therefore, recommended expressions for the present test sections [2] were used.

The correlation equation of Li *et al.* [9] was compared to the present data. The equation of Li *et al.* was based on data obtained exclusively from spirally indented tubes and the data nearly covered the e/D and p/D range of this study. The equation does not reduce to the smooth tube case as e/D approaches zero. Consequently, the predictions are invalid at small values of e/D and the comparisons with data were poor for $e/D < 0.021$.

Rabas *et al.* [2] developed a correlation from a data base (subset of data base [13]) specific to spirally indented tubes. The data base of ref. [2] included the data of both Withers [8] and Li *et al.* [9]. The correlation of Rabas *et al.* [2] simplifies to Blasius equation as e/D approaches zero and the general agreement with all of the data of this study was considered reasonable.

The best predictions of the friction factor data of this study were obtained from the correlation [1] based on a variety of geometries similar to the indented surface. The data comparison is shown in Fig. 9 and the large pitch data of ref. [1] are included (solid symbols). The data of ref. [1] and the data of the present study are seen to be in good agreement and the friction factor correlation of ref. [1] is

$$f/f_s = (1+Z^{15/16})^{16/15} \tag{11}$$

where

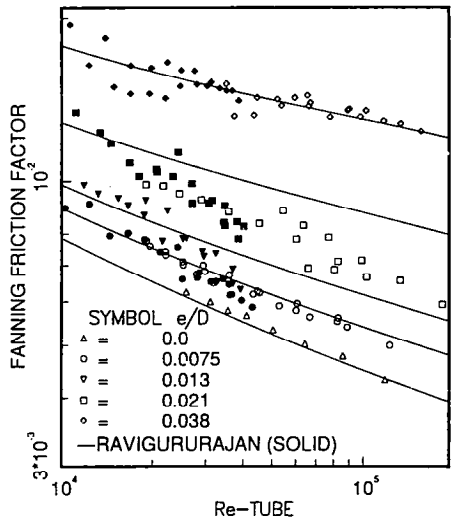

FIG. 9. The Fanning friction factor as a function of Reynolds number and indentation height.

$$f_s = (1.58\ln(Re) - 3.28)^{-2} \tag{12}$$

and

$$Z = 29.1\, Re^{R_1}(p/D)^{R_2}(e/D)^{R_3}(\alpha/90)^{R_4}(1+2.94/n)\sin\beta \tag{13}$$

where

$$R_1 = 0.67 - 0.06(p/D) - 0.49(\alpha/90) \tag{14}$$

$$R_2 = -1.66\times10^{-6}\,Re - 0.33(\alpha/90) \tag{15}$$

$$R_3 = 1.37 - 0.157(p/D) \tag{16}$$

$$R_4 = 4.59 + 4.11\times10^{-6}\,Re - 0.15(p/D). \tag{17}$$

Equation (11) simplifies to a plain tube equation as the indentation height, e, tends to zero. The good agreement with the plain tube data of this study shown in Fig. 9 is an indication of the accuracy of the measurements. (These data agree even better with the Blasius equation.)

Many investigations have applied the friction similarity function of ref. [10] to rough surface tubes. In an earlier work, Webb *et al.* [11] applied the following function to transverse indented tubes:

$$R = \left(\frac{2}{f}\right)^{0.5} + 2.5\ln(2e/D) + 3.75. \tag{18}$$

This function is compared to the large pitch data in Fig. 10. The data exhibit distinct trends as a function of indentation height, e/D. The smallest indentation height tested, $e/D = 0.0075$ at the largest pitch to height ratio, $p/e = 120$, behaved like a perturbation on the plain tube results ($r = 2.5\ln(e^+) + 5.5$). The dependence on roughness Reynolds number, e^+, is seen in Fig. 10. The results show that even at the smallest value studied, $p/e = 24$, the friction data indicate that the fully rough region was not reached as the dependence on e^+ was still present. This trend was

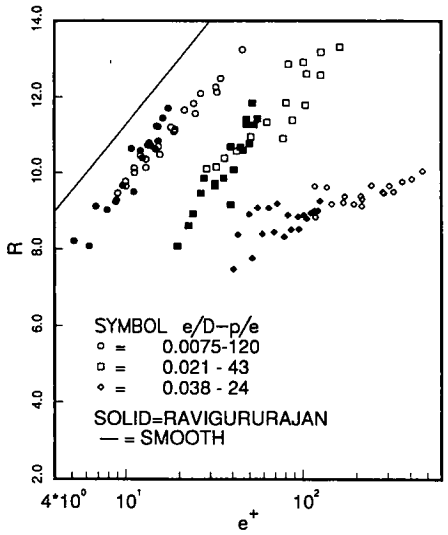

FIG. 10. Friction similarity parameter as a function of roughness Reynolds number.

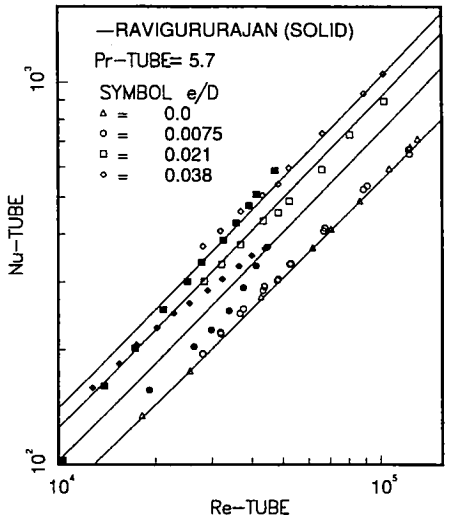

FIG. 11. The tube-side heat-transfer coefficient as a function of Reynolds number and indentation height.

observed [12] in spirally indented tubes with p/e in the range of 10–50. The data of ref. [12] were correlated by the parameter $R(e/p)^{0.53}$, which agreed with the present data reasonably well for $p/e = 24$ and 43, but the largest $p/e = 120$, which is outside the range of the work of ref. [12], was not correlated by this parameter.

A final friction factor comparison was made with the correlation of Nakayama *et al.* [13]. The tubes in this work were not indented, spiral ribs were used and a p/e as large as 56.7 was tested. The friction factor data, which showed some consistency with Withers' data, were correlated by the function $(R-4.5)(e/p)^{2.59}$. This function did not extrapolate well to the large pitch data of this study. It is evident in Fig. 9 that the fully rough condition is being approached from a negative slope of the f vs Re curve as compared to indented tubes with small p/e where this condition approaches from a positive slope.

Tube heat transfer

Heat transfer results for the tubes tested are shown in Fig. 11 at $Pr = 5.7$. This is the only Prandtl number at which there is overlapping data from ref. [1] and those data are included in Fig. 11 along with the heat-transfer correlation predictions of ref. [1]. Predictions of the present data are good except at the lowest indentation height tested, $e/D = 0.0075$. The present data were predicted within an error band of approximately 25% with the data tending to be overpredicted. The data of ref. [1] were not as well predicted, nor were the trends. These data were obtained using the direct tube-wall heating approach and were subject to the experimental difficulties discussed in the introduction.

In an attempt to find a more accurate prediction of the current data for spirally indented tubes, Nusselt number correlations were investigated from the sources used for friction factor comparisons. The Rabas *et al.* [2] equation for Nusselt number, developed exclusively from spirally indented tubes, predicted the present data reasonably. Although there was a tendency to underpredict the data, there were no systematic errors and the data were all within a 20% error band. The semi-empirical equation of Rabas *et al.* [2] is

$$Nu = 0.027E_h\, Re^{0.8}\, Pr^{1/3} \tag{19}$$

where the heat-transfer enhancement factor is

$$E_h = 1 + \frac{1.182F_1F_2}{(p/D)^{0.046}}. \tag{20}$$

The factors F_1 and F_2 are functions of indentation height and pitch, respectively. They are

$$F_1 = \exp\left\{-\sum_{i=1}^{4} C_i\left[\ln\left(\frac{e}{D}\right)\right]^{i-1}\right\} \tag{21}$$

$$F_2 = \cos\tan^{-1}\left(\frac{p/D}{\pi}\right). \tag{22}$$

The constants are: $C_1 = 5.077$, $C_2 = 4.422$, $C_3 = 1.124$ and $C_4 = 0.06760$. (Below an indentation height of $e/D = 0.0002$, the factor F_1 should be set equal to 0.0 in equation (20).)

Equation (19) is a modification of earlier work [14]. Comparing the prediction of ref. [14] with the present data, the Rabas *et al.* equation was found to present a slight improvement over the previous correlation [14].

Other heat-transfer correlations that were based on the heat-transfer similarity functions shown below were examined

$$G = \left(\frac{f}{2St} - 1\right)\Big/(f/2)^{0.5} + R. \tag{23}$$

This function is based on the analogy between heat and momentum transfer in rough tubes characterized by e/D. Use of G with the present data and the roughness Reynolds number, e^+, exhibited the potential for successful correlation of the large pitch data. As a minimum, a Prandtl number dependence was required for correlation. The function e^+ is

$$e^+ = \left(\frac{e}{D} Re \left(\frac{f}{2}\right)^{0.5}\right). \quad (24)$$

Nakayama *et al.* [13] found the correlation of Webb *et al.* [11] predicted their data well indicating that heat transfer is less sensitive to the indentation shape and orientation than is friction factor. Webb *et al.* employed a Prandtl number dependence to the power of -0.57 and this result was applied to the current data. The large pitch data were not well predicted; systematic errors occurred as a function of indentation height and the data extended well outside of a 20% error band. In evaluating the function, G and e^+, the friction factor was calculated from equation (11) which was shown to be the best representation of the present data. Data comparisons were worse when the friction factor of ref. [13] was used.

The heat-transfer coefficients due to Withers [8] and Li *et al.* [9] were compared to the present data. The correlations did not predict the large pitch data well even using the friction factor of equation (11). All of the data were overpredicted by Withers' equation and underpredicted by the equation of Li *et al.* Although the predicted Nusselt numbers were poor in terms of magnitude, both correlations predicted the data trend reasonably well, and the data scatter was not large which is supportive of the analogy correlating approach.

The best predictions of the present data, from the analogy type correlations considered, came from ref. [12]. An explicit pitch dependence was employed, and the correlating parameter showed good agreement with the magnitudes and trends of the data as shown in Fig. 12. The data were predicted within a 20% error band using equation (11) for friction factor. Some systematic error is observed in Fig. 12 where the lowest indentation height data are consistently overpredicted. The Mehta and Raja Rao correlation [12] is shown below

$$G\,Pr^{-0.55}\frac{p^{0.15}}{D} = 9.4(e^+)^{0.11}. \quad (25)$$

Combined heat transfer and friction

The ratio of enhanced tube-side Nusselt number to plain-tube Nusselt number was divided by the ratio of enhanced-tube friction factor to plain-tube friction factor to form the enhancement efficiency index. A typical set of results is shown in Fig. 13. The plain-tube Nusselt number was calculated from the Petukhov–Popov [5] equation using the plain-tube friction factor that compared well with the data of this study. The

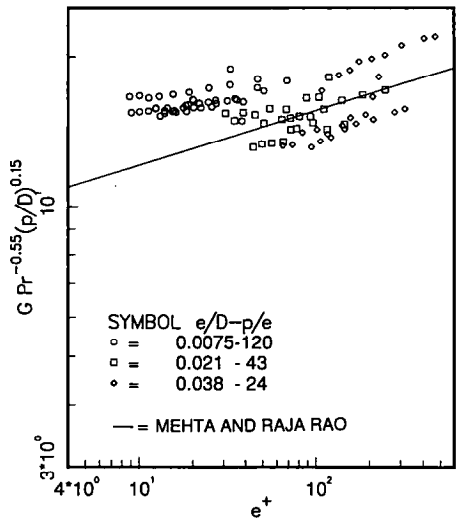

FIG. 12. The heat transfer similarity parameter as a function of roughness Reynolds number.

ratio of the enhanced-tube friction factor to the plain-tube friction factor was calculated from equation (11) which also compared well with the present data. The trend of Fig. 13 is consistent with the results of Webb *et al.* [11]. The effect of indentation height, e/D, is to reduce the efficiency index, and at larger Prandtl numbers the index approaches (and may exceed) unity at small values of e^+. The magnitudes of these indices are also in the range of the results of Webb *et al.*

The efficiency index of Fig. 13 should be viewed with respect to the actual heat-transfer performance. The heat-transfer enhancement was approximately 10% at e/D of 0.0075, 50% at $e/D = 0.021$ and 100% at $e/D = 0.038$ ($Pr = 8.8$). This heat-transfer enhancement exhibited a clear Prandtl number dependence at the largest indentation height tested, increas-

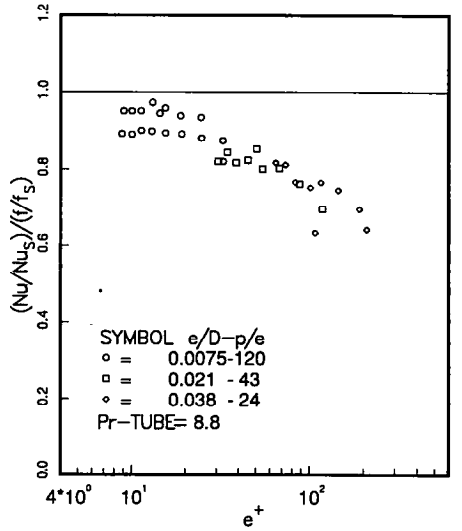

FIG. 13. The enhancement efficiency index as a function of roughness Reynolds number.

ing with Prandtl number in a manner similar to that reported [11]. The heat-transfer enhancement for the spirally indented tube with $e/D = 0.038$ ranged from 50% at $Pr = 3.6$ to 100% at $Pr = 8.8$. At the higher Prandtl numbers, the indentations extended well into the thermal boundary layer which could account for this observation.

Mehta and Raja Rao [12] showed data that exhibit a tendency to produce peaks in the efficiency index as a function of roughness Reynolds number. This result for any given enhanced tube implies that the Reynolds number exponent, γ, decreases with increasing Reynolds number. For the large p/e ratios of this study, such peaking tendency was essentially not observed. The data reduction technique did show that γ decreased with increasing indentation height, e/D. The data reduction technique used did not mask any dependence of γ on Reynolds number since γ was used only in evaluation of the annulus heat-transfer coefficient as discussed previously.

The dependence of the Reynolds number exponent, γ, on indentation geometry, height or pitch, was seen in the results of ref. [15]. The data reduction technique used for the heat exchanger test unit of that study did not iterate on assumed values of γ as in the present study. Instead, a computer optimization routine determined the value for each test series. The p/e ratio was less than 18 for the tests of ref. [15], and consequently no direct comparison with the present data was made. The present results showed a dependence of γ on the enhanced tube geometry but not on the Reynolds number. It is noteworthy that an optimization technique similar to that of ref. [15] was attempted in the early stages of this study. It was found that constraints on optimization were required to dampen sensitivity to small errors in the data. This requirement was, in effect, the same as iterating on the range of γ as done in the data reduction technique eventually adopted.

CONCLUSIONS

The data reduction technique developed was verified against plain tube data assuming that the exponent on Reynolds number for Nusselt number dependence was unknown. This technique was then applied to the spirally indented tube test sections. The Reynolds number exponents for both inside and annulus flows were found to be nearly equal ($\gamma = \delta$). This condition was a result of optimizing the data reduction technique to the present set of data and is not a necessary condition for applying the technique to a new situation. It should be emphasized that once an annulus heat-transfer coefficient was determined using this technique, the evaluation of the tube or inside heat-transfer coefficient was independent of γ and δ. It is concluded that this data reduction technique used with a heat exchanger test unit provides a viable means of determining enhanced surface heat-transfer coefficients for heat exchanger application. Observation of $\gamma = \delta$ suggests that the heat-transfer enhancement is governed by similar flow separation and reattachment mechanisms.

The friction factor results of the large pitch spirally indented tubes of this study were in good agreement with data of ref. [1]. The friction similarity function, that has been used successfully as the basis of friction factor correlations for other rough surfaces, produced consistent trends with the present data; however, they did not quantitatively predict the present data. The more empirical approach [1] produced the best agreement with the present experimental friction factors. However, the potential for improved accuracy using the similarity function approach was indicated.

Application of the literature heat-transfer correlations to the large p/e ratios of this study resulted in identification of the two correlations producing good results: the semi-empirical relation [2] and the result based on the heat and momentum transfer analogy [12]. The latter used a heat-transfer similarity function and the potential for further improvement in accuracy by pursuing this approach was indicated in the data presented. These two correlations are based on the analogy approach which requires accurate values of the friction factor.

A maximum heat-transfer enhancement value of 100% was achieved; however, no peak was observed in this enhancement as a function of Reynolds number as reported in the literature for low pitch enhanced tubes. A Prandtl number dependence was seen clearly at large indentation heights and the efficiency index decreased with indentation height from a value approaching unity at very small e/D. This general behavior produced relatively low friction factors with moderate heat-transfer enhancement that would be desirable for application to pressure drop sensitive systems.

Acknowledgement—This work was supported by the U.S. Department of Energy, Assistant Secretary for Conservation and Renewable Energy, Wind/Hydro/Ocean Technologies Division, under contract W-31-109-Eng-38.

REFERENCES

1. T. S. Ravigururajan and A. E. Bergles, Study of water-side enhancement for ocean thermal energy conversion heat exchangers, Technical Report, Iowa State University, Engineering Research Institute, HTL-44 (December 1986).
2. T. J. Rabas, A. E. Bergles and D. L. Moen, Heat transfer and pressure drop correlation for spirally indented (rope) tubes used in surface condensers and multistage flash evaporators, *Proc. 1988 Heat Transfer Conf.*, ASME, HTD-96, Vol. 1, pp. 693–704 (July 1988).
3. E. E. Wilson, A basis for rational design of heat transfer apparatus, *Trans. Am. Soc. Mech. Engrs* **37**, 47–82 (1915).
4. L. Seren, C. B. Panchal and D. M. Rote, Temperature sensors for OTEC applications, ANL/OTEC-PS-12 (May 1984).
5. B. S. Petukhov, Heat transfer and friction in turbulent

pipe flow with variable physical properties, *Adv. Heat Transfer* **6**, 503 (1970).
6. C. C. Monrad and J. F. Pelton, Heat transfer by convection in annular spaces, *Trans. A.I.Ch.E.* **38**, 593 (1942).
7. J. G. Knudsen and D. L. Katz, *Fluid Dynamics and Heat Transfer*. McGraw-Hill, New York (1958).
8. J. G. Withers, Tube-side heat transfer and pressure drop for tubes having internal ridging with turbulent/traditional flow of single-phase fluid, Part 1, single-helix ridging, *Heat Transfer Engng* **2**(1), 48–58 (1980).
9. H. M. Li, K. S. Ye, Y. K. Tan and S. J. Den, Investigation of tube-side flow visualization, friction factor, and heat transfer characteristics of helical-ridging tubes, *Proc. 7th Int. Heat Transfer Conf.*, Vol. 3, pp. 75–80. Hemisphere, New York (1982).
10. D. F. Dipprey and R. H. Sabersky, Heat and momentum transfer in smooth and rough tubes at various Prandtl numbers, *Int. J. Heat Mass Transfer* **6**, 329–353 (1963).
11. R. L. Webb, E. R. G. Eckert and R. J. Goldstein, Heat transfer and friction in tubes with repeated rib roughness, *Int. J. Heat Transfer* **14**, 601–617 (1971).
12. M. H. Mehta and M. Raja Rao, Analysis and correlation of turbulent flow heat transfer and friction coefficients in spirally corrugated tubes for steam condenser application, *Proc. 1988 Heat Transfer Conf.*, ASME, HTD-96, Vol. 3, pp. 307–312 (July 1988).
13. W. Nakayama, H. Takahashi and T. Daikoku, Spiral ribbing to enhance single-phase heat transfer inside tubes, *Proc. ASME–JSME Thermal Engng Joint Conf.*, Honolulu, Hawaii, pp. 365–372 (1983).
14. Yorkshire Imperial Metals, YIM heat exchanger tubes; design data for horizontal rope tubes in steam condensers, Technical Memorandum 3, Yorkshire Imperial Metals, Ltd, Leeds, England (1982).
15. Y. Goth, M. Feidt, F. Lauro et A. Bailly, Transferts de Chaleur et Pertes de Charge en Ecoulement Monophasique Eau–Eau et les Tubes Corrugues, *Revue Gen. Thermique* **294–295**, 341–348 (June–July 1986).